Bearing capacity of spatially random cohesive soil using numerical limit analyses

Kasama, Kiyonobu
Division of Civil and Structural Engineering, Faculty of Engineering, Kyushu University

Whittle, Andrew J.
Department of Civil and Environmental Engineering, Massachusetts Institute of Technology

出版情報：Journal of Geotechnical and Geoenvironmental Engineering. 137 (11), pp.989-996, 2011-11. American Society of Civil Engineers
バージョン：

Bearing Capacity of Spatially Random Cohesive Soil Using Numerical Limit Analyses

by

Kiyonobu Kasama[1] and Andrew J. Whittle[2], M.ASCE

ABSTRACT: This paper describes a probabilistic study of the two dimensional bearing capacity of a vertically loaded strip footing on spatially random, cohesive soil using Numerical Limit Analyses (NLA-CD). The analyses use a Cholesky Decomposition technique to represent the spatial variation in undrained shear strength within finite element meshes for both upper and lower bound analyses, assuming an isotropic correlation length. Monte Carlo simulations are then used to interpret the bearing capacity for selected ranges of the coefficient of variation in undrained shear strength and the ratio of correlation length to footing width. The results are compared directly with data from a very similar study by Griffiths et al. in which bearing capacity realizations were computed using a method of Local Average Subdivision (LAS) in a conventional displacement-based Finite Element Method (FEM-LAS). These comparisons show the same qualitative features, but suggest that the published FEM calculations tend to overestimate the probability of failure at large correlation lengths. The NLA method offers a more convenient and computationally efficient approach for evaluating effects of variability in soil strength properties in geotechnical stability calculations.

Keywords: Bearing capacity; cohesive soil, limit analysis; Monte Carlo method; Random field, Probabilistic analysis

---

[1] Research Associate, Division of Civil and Structural Engineering, Faculty of Engineering, Kyushu University, Fukuoka, Japan.

[2] Professor, Department of Civil and Environmental Engineering, Massachusetts Institute of Technology, Cambridge, MA.

Introduction

Recent numerical formulations of upper and lower bound limit analyses for rigid perfectly plastic materials, using finite element discretization and linear (Sloan, 1988a; Sloan & Kleeman, 1995) or non-linear (Lyamin & Sloan, 2002a, b) programming methods, provide a practical, efficient and accurate method for performing geotechnical stability calculations. For example, Ukritchon et al. (1998) proposed a solution to the undrained stability of surface footings on non-homogeneous and layered clay deposits under the combined effects of vertical, horizontal and moment loading to a numerical accuracy of ±5%. The only parameter used in these NLA is the undrained shear strength (which can vary linearly within a given soil layer). Hence, NLA provides a more convenient method of analyzing stability problems than FEM's which also require the specification of elastic stiffness parameters and simulation of the complete non-linear load-deformation response up to collapse.

This paper investigates a probabilistic approach to evaluating the bearing capacity of a planar footing on clay by incorporating the stochastic spatial variability of undrained shear strength within the numerical limit analyses. The undrained shear strength is treated as a random field (Vanmarcke, 1984) which is characterized by a log-normal distribution and a spatial correlation length (i.e., isotropic correlation structure). The current calculations use a Cholesky Decomposition technique (Baecher & Christian, 2003) to incorporate these random properties in numerical limit analyses (NLA-CD). The bearing capacity is then interpreted statistically from a series of Monte Carlo simulations.

Very similar studies have been reported by Griffiths and Fenton (2001) and Griffiths et

al. (2002) using displacement-based finite element analyses (FEM) with Local Area Subdivision (after Fenton & Vanmarcke, 1990) to represent random distributions of shear strength (FEM-LAS). The current paper adopts similar notations and provides a direct comparison of results from the two methods of analysis.

Numerical Limit Analysis with Spatially Random Cohesive Soil

Figures 1 illustrate typical finite element meshes used to compute upper and lower bounds on the two dimensional bearing capacity of a vertically loaded plane strain footing of width, B. The lower bound analyses is based on the linear programming formulation presented by Sloan (1988a) and assume a linear variation of the unknown stresses (σ_x, σ_y, τ_{xy}) within each triangular element. The formulation differs from conventional displacement-based finite-element formulations by assigning each node uniquely within an element, such that the unknown stresses are discontinuous along adjacent edges between elements. Statically admissible stress fields are generated by satisfying: i) a set of linear equality constraints, enforcing static equilibrium with triangular elements and along stress discontinuities between the elements, ii) inequality constraints that ensure no violation of the linearized material failure criterion. The current analyses assume a Tresca yield criterion for the undrained shear strength of clay. The lower-bound estimate of the collapse load is then obtained through an objective function that maximizes the resultant vertical force acting on the footing. The linear programming problem is solved efficiently using a steepest edge active set algorithm (Sloan, 1988b).

The upper-bound formulation also discretizes the soil mass into three-noded triangular elements, Figure 1, with linear variations in the unknown velocities (u_x, u_y). Nodes are unique

to each element and hence, the edges between elements represent planes of velocity discontinuities. Plastic volume change and shear distortion can occur within each element as well as along velocity discontinuities. The kinematic constraints are defined by the compatibility equations and the condition of associated flow (based on an appropriate linearization of the Tresca criterion) within each element and along the velocity discontinuities between elements. The external applied load can be expressed as a function of unknown nodal velocities and plastic multiplier rates. The upper-bound on the collapse load can then be formulated as a linear programming problem, which seeks to minimize the external applied load using an active set algorithm (after Sloan & Kleeman, 1995).

One of the principal advantages of NLA is that the true collapse load is always bracketed by results from the upper and lower bound calculations. However, careful mesh refinement is essential in order to achieve numerically accurate solutions. Sloan (1988a) and Sloan & Kleeman (1995) have reported the influence of mesh refinement and approximation of linearized Tresca criterion in the lower bound and upper bound numerical limit analyses respectively. Based on prior studies by Ukritchon et al. (1998), the current upper bound analyses use a uniform mesh with elements of characteristic dimension 0.125B, Figure 1. The size of the discretized domain is sufficient to contain all potential failure mechanisms, such that the far field boundaries can be represented as zero velocity conditions. Extension elements are introduced in order to ensure statically admissible solutions at all points in the deep clay layer (half-space).

The effects of inherent spatial variability are represented in the analyses by modeling the undrained shear strength, s_u, as a homogeneous random field while the effect of the spatial variability of soil density is neglected by assuming the soil to be weightless. The undrained shear strength is assumed to have an underlying log-normal distribution with mean, μ_{s_u}, and

standard deviation, σ_{s_u}, and an isotropic scale of fluctuation (also referred to as the correlation length), $\theta_{\ln s_u}$. The use of the log-normal distribution is predicated by the fact that s_u is always a positive quantity. Phoon and Kulhawy (1999) have compiled data on the inherent variability of s_u and report typical Coefficients of Variation in undrained shear strength, $COV_{s_u} = \sigma_{s_u} / \mu_{s_u}$ = 0.1 – 0.8, based on conventional laboratory shear tests. The mean and standard deviation of logs_u are readily derived from COV_{s_u} and μ_{s_u} as follows (e.g., Baecher & Christian, 2003):

$$\sigma_{\ln s_u} = \sqrt{\ln(1 + COV_{s_u}^2)} \tag{1}$$

$$\mu_{\ln s_u} = \ln \mu_{s_u} - \frac{1}{2}\sigma_{\ln s_u}^2 \tag{2}$$

There is much less data available to evaluate the scale of fluctuation which corresponds to the physical distance over which there is correlation in the undrained shear strength. Although some studies have found that the horizontal scale of fluctuation can be an order of magnitude greater than the vertical scale (e.g., James Bay marine clay deposits; DeGroot & Baecher, 1983), the local geological environment is likely to have a major influence on the correlation length parameter(s). Following Griffiths et al. (2002) the current analyses present results based on assumed values of the ratio of the correlation length to footing width, $\Theta_{\ln s_u} = \theta_{\ln s_u} / B$.

The spatial variability is incorporated within the NLA meshes by assigning the undrained shear strength corresponding to the i^{th} element:

$$s_{u_i} = \exp(\mu_{\ln s_u} + \sigma_{\ln s_u} G_i) \tag{3}$$

where G_i is a random variable that is linked to the spatial correlation length, $\theta_{\ln s_u}$.

Values of G_i are obtained using a Cholesky Decomposition technique (e.g., Baecher &

Christian, 2003) using an isotropic Markov function which assumes that the correlation decreases exponentially with distance between two points *i, j* :

$$\rho(x_{ij}) = \exp\left\{-\frac{2x_{ij}}{\theta_{\ln s_u}}\right\} \tag{4}$$

where ρ is the correlation coefficient between two random values of s_u at any points separated by a distance $x_{ij} = |\boldsymbol{x}_i - \boldsymbol{x}_j|$ where $\boldsymbol{x}_i$ is the position vector of i (located at the center of element i in the finite element mesh). This correlation function can be used to generate a correlation matrix, $\boldsymbol{K}$, which represents the correlation coefficient between each of the elements used in the NLA finite element meshes:

$$\boldsymbol{K} = \begin{bmatrix} 1 & \rho_{12} & \cdots & \rho_{1n} \\ \rho_{12} & 1 & \cdots & \rho_{2n} \\ \vdots & \vdots & \ddots & \vdots \\ \rho_{1n} & \rho_{2n} & \cdots & 1 \end{bmatrix} \tag{5}$$

where ρ_{ij} is the correlation coefficient between element i and j, and n the total number of elements in the mesh.

The matrix $\boldsymbol{K}$ is positive definite and hence, the standard Cholesky Decomposition algorithm can be used to factor the matrix into triangular forms used in NLA mesh, $\boldsymbol{S}$ and $\boldsymbol{S}^{\mathrm{T}}$, respectively:

$$\boldsymbol{S}^T\boldsymbol{S} = \boldsymbol{K} \tag{6}$$

The components of $\boldsymbol{S}^T$ are specific to a given finite element mesh and selected value of the correlation length, $\theta_{\ln s_u}$.

The vector of random variables, $\boldsymbol{G}$ (i.e., $\{G_1, G_2, \cdots, G_n\}$, where G_i specifies the random component of the undrained shear strength in element i, eqn. 3) can then be obtained from the product:

$$\boldsymbol{G} = \boldsymbol{S}^T \boldsymbol{X} \tag{7}$$

where $\boldsymbol{X}$ is a vector of statistically independent, random numbers $\{x_1, x_2, \cdots, x_n\}$ with a standard normal distribution (i.e., with zero mean and unit standard deviation). It is noted that undrained shear strength calculated at the center of element is used as an input strength parameter to the each element in NLA mesh. Namely, it is assumed in this paper that the strength of entire element can be represented by the strength at the center of element, which is expected that the accuracy of spatial correlation relationship by Cholesky Decomposition technique is affected by the mesh size for NLA.

In order to investigate the accuracy and mesh dependency of spatial correlation relationship obtained by Cholesky Decomposition technique, Figure 2 shows the comparison of exact correlation, which is an exponential function as Equation (4), and realized correlation in NLA mesh (Figure 1) calculated by Cholensky Decomposition technique. It is noted that the plot interval for markers by Cholensky Decomposition technique in Figure 2 is 0.05B, which is almost equal to a minimum distance between the element centers in NLA mesh. It can be seen that there are good agreements between exact correlation lines and plot markers calculated by Cholensky Decomposition technique. However, the comparatively rough realization of exact correlation relation for $\Theta_{\ln s_u} = 0.1$ ($\theta_{\ln s_u} = 0.1$B) is obtained, which is suggested that the element size for NLA analyses is should be small for this case. Namely, it can be suggested that the element size is at least the half of spatial correlation length when using Cholesky Decomposition technique for realizing spatial correlation structure in finite element mesh. Therefore, it is confirmed that Cholesky Decomposition technique for fine NLA mesh is a useful method to obtain random field parameters with a good accuracy.

Values of the random variable vector $\boldsymbol{X}$ are then re-generated for each realization in a set

of Monte Carlo simulations. Figures 1 illustrate the spatial distribution of undrained shear strength obtained for typical mesh for one example simulation with input parameters μ_{s_u} =100kPa,. COV_{c_u} = 0.2 and $\Theta_{\ln s_u}$ = 1.0. The lighter shaded regions indicate areas of higher shear strength.

Bearing Capacity Results

Upper and lower bound stability calculations have been performed assuming a fixed mean value for the undrained shear strength, μ_{s_u} =100kPa, while varying combinations of the coefficient of variation and correlation length over the following ranges:

COV_{s_u} = 0.2, 0.4, 0.6, 0.8, 1.0, 4.0

$\Theta_{\ln s_u}$ = 0.1, 0.2, 1.0, 2.0, 4.0, 8.0, 20

Figure 3 illustrates the effects of the correlation length parameter on the mechanisms of failure from a series of three UB simulations with COV_{s_u} = 0.4 and $\Theta_{\ln s_u}$ = 0.2, 1.0, 2.0. Each example shows the specific realization of the undrained strength field superimposed on the deformed FE mesh, together with the vectors of the computed velocity field (dark shaded regions in these figures represent locations where plastic distortion occurs within the finite elements). The strength field appears ragged for $\Theta_{\ln s_u}$ =0.2, but is much smoother. for $\Theta_{\ln s_u}$ = 1.0, 2.0. Close inspection shows that the computed failure mechanisms find paths of least resistance, passing through weaker regions of the clay.

A series of 1000 Monte Carlo simulations have been performed for each combination of the input parameters (COV_{s_u}, $\Theta_{\ln s_u}$). The computed bearing capacity factor, N_{ci}, can then be reported for each realization of the shear strength field:

$$N_{ci} = q_{fi} / \mu_{s_u}, \qquad \text{where } i = 1,2,\ldots n \ldots 1000 \tag{8}$$

where q_{fi} is the computed collapse load (either UB or LB).

The mean, μ_{N_c}, and standard deviation, σ_{N_c}, of the bearing capacity factor are recorded through each set of Monte Carlo simulations, as follows:

$$\mu_{N_c} = \frac{1}{n}\sum_{i=1}^{n} N_{ci}; \quad \sigma_{N_c} = \sqrt{\frac{1}{n-1}\sum_{i=1}^{n}(N_{ci} - \mu_{N_c})^2}. \tag{9}$$

Figure 4 illustrates one set of results for the case with $\Theta_{\ln s_u} = 2.0$, $COV_{s_u} = 0.2$ and 0.8. The results confirm that the collapse load for any given realization is well bounded by μ_{N_c} from the UB and LB calculations. The mean and standard deviation of N_c become stable within 1000 simulations.

Table 1 summarizes the statistical data for the bearing capacity factor for all combinations of the input parameters. In all cases the results show $\mu_{N_c}(UB) > \mu_{N_c}(LB)$, the actual collapse load is typically bounded within ±5-10% showing acceptable accuracy from the numerical limit analyses. The data also show $\sigma_{N_c}(UB) > \sigma_{N_c}(LB)$. This latter result may reflect differences in the upper bound and lower bound limit analyses. However, it is notable that the numerical limit analyses generate much smaller coefficients of variation in bearing capacity than were reported by Griffiths et al. (2002) from FEM-LAS simulations (the data in Table 1 show $COV_{N_c} = \sigma_{N_c} / \mu_{N_c} = 0.03 - 0.75$).

Figure 5 presents a 20-bin histogram of the bearing capacity factor from one complete series of Monte Carlo simulations with $COV_{s_u} = 0.2$ and $\Theta_{\ln s_u} = 2.0$ together with the estimated normal distribution. In order to obtain the distribution function of the bearing capacity factor based on χ^2 goodness-of-fit tests, Table 1 summarizes χ^2 statistics for all of the simulations

and confirms that normal or log-normal distribution functions can be used to characterize the bearing capacity at a 5% significance level (with acceptance level, $\chi^2_{20-1-2}[0.05] = 27.6$).

Figures 6a and 6b summarize the ratio of the mean bearing capacity factor to the deterministic solution for homogeneous clay, $\tilde{N}_c = \mu_{N_c} / N_{cDet}$ (where $N_{cDet} = [2+\pi]$) for combinations of the input parameters (COV_{s_u}, $\Theta_{\ln s_u}$). In general, $\tilde{N}_c < 1$ and hence spatial variability causes a reduction in the expected undrained bearing capacity. The trends show that the largest reductions in μ_{s_u} occur when the coefficient of variation is high and/or the correlation length is small. Assuming a maximum realistic range, $COV_{s_u} \leq 0.6 - 0.8$, the results suggest that the expected bearing capacity could be as little as 60% of the deterministic value.

Qualitatively similar results have been presented by Griffiths et al. (2002). However, these Authors also report a local minimum in the expected bearing capacity for $\Theta_{\ln s_u} \approx 1.0$, which is not seen in the current numerical limit analyses. It is also shown that the differences between current UB and LB analyses is large for small $\Theta_{\ln s_u}$. It is considered that the difference of these bearing capacities obtained by NLA-CD and FEM-LAS for small $\Theta_{\ln s_u}$ is related to the mesh dependency of spatial correlation relation obtained by Cholesky Decomposition technique as explained in Figure 2.

Probability of Failure

In conventional working stress design practice an average undrained shear strength is used to compute the ultimate bearing capacity, while the allowable/nominal load is then obtained by applying a global safety factor, $FS = 2.0 - 3.0$. In the current calculations the probability that the bearing capacity is less than a given level of applied load can be obtained by assuming that N_c

can be described by either a normal or log-normal distribution (as shown in Table 1). If N_c is log-normally distributed, the probability that the bearing capacity is less than the nominal load is given by:

$$P[N_c < N_{cDet} / FS] = \Phi\left(\frac{\ln([2+\pi]/FS) - \mu_{\ln N_c}}{\sigma_{\ln N_c}} \right) \qquad (10)$$

where $\Phi(..)$ is the cumulative normal function and values of $\mu_{\ln N_c}$, $\sigma_{\ln N_c}$ are reported from the NLA-DC analyses in Table 1.

Figure 7 summarizes predictions that the probability of bearing failure is less than the nominal load level for FS = 1.0, 2.0 and 3.0 as functions of the coefficient of variation in undrained shear strength, COV_{s_u}, for correlation length parameters, $\Theta_{\ln s_u}$ = 1.0, 2.0 and 4.0. As expected, when spatial variability is included in the analyses, the ultimate bearing capacity is almost always less than the deterministic capacity based on the mean shear strength. The LB solutions show that the probability of this event ($P[N_c < N_{cDet}]$) is greater than 0.90 (for all cases considered), while Upper Bound solutions find $P > 0.66$. These results can be compared directly with earlier solutions from FEM-LAS reported by Griffiths et al. (2002) who find $P > 0.55$ (for the same range of input parameters).

The probability that the bearing capacity is less than the nominal design load for FS = 2.0 and 3.0 decreases very markedly with the coefficient of variation in undrained shear strength, especially for $COV_{s_u} < 1.0$, Figure 7, and also with increasing values of the spatial correlation length ratio, $\Theta_{\ln s_u}$.

For $\Theta_{\ln s_u} = 1.0$, the UB predictions of the probability, $P[N_c < N_{cDet}/FS]$ are in excellent agreement with prior data presented by Griffiths et al. (2002). However, the current analyses

show lower event probabilities for correlation length ratios, $\Theta_{\ln s_u} = 2.0, 4.0$. The source of this discrepancy is not obvious and deserves further investigation.

Figure 8 offers a more detailed comparison of the probability of bearing failure implicitly defined in conventional design methods with the actual probabilities of failure derived from the stochastic NLA-CD analyses accounting for inherent spatial variability. The figures plot the $P[N_c < N_{cDet}/FS]$ as functions of the safety factor, FS for selected ranges of the input parameters COV_{s_u} and $\Theta_{\ln s_u}$. The target probabilities of failure considered in LRFD codes for shallow foundations are reported in the range, $P_f = 10^{-2} - 10^{-3}$ (Baecher & Christian, 2003; Phoon et al., 2000). The results in Figure 8a show that $P[N_c < N_{cDet}/FS]$ is much less than this target condition for small values of the coefficient of variation, $COV_{s_u} = 0.2$. There is close agreement between the conventional working stress design and LFRD methods for $COV_{s_u} = 0.4$, 0.6, Figures 8b, c. However, in exceptional cases with $COV_{s_u} = 0.8$ and $\Theta_{\ln s_u} \leq 1.0$, the estimated probability of failure can exceed $P_f = 10^{-2}$ at $FS = 3.0$.

Conclusions

This paper summarizes the implementation of a Cholesky Decomposition method for representing inherent spatial variability of undrained shear strength in Monte Carlo simulations of bearing capacity for a rough, surface strip footing on clay using Numerical Limit Analyses. Accurate estimates of the exact bearing capacity are achieved in each Monte-Carlo realization except for small spatial correlation length. The analyses assume that undrained shear strength is characterized by a log-normal distribution function, while effects of spatial variability are characterized by two input parameters, i) the coefficient of variation, COV_{s_u} and ii) an

isotropic correlation length ratio, $\Theta_{\ln s_u}$. Stable bearing capacity statistics were derived from a series 1000 Monte Carlo simulations for each set on input parameters. The current parametric calculations are then compared with results from a similar study reported by Griffiths et al. (2002) using a completely independent method of analysis (FEM-LAS).

The results confirm that spatial variability reduces the bearing capacity of the footing relative to a deterministic calculation based on the mean undrained shear strength. This result occurs due to changes in the predicted failure mechanisms which form through weaker regions in the clay. The lowest values in the computed ratio, $\tilde{N}_c = \mu_{N_c} / N_{cDet}$, occur at high values of COV_{s_u} and small correlation length ratios ($\Theta_{\ln s_u} < 1$) in this analyses.

Although there is very good qualitative agreement with results presented by Griffiths et al. (2002) the current analyses generally suggest lower probabilities of design failure for the same input properties of the undrained shear strength field. This result will require further investigation through direct comparison of stochastic NLA and FEM methods.

The results suggest that target probabilities for bearing failure in the range $P_f = 10^{-2} - 10^{-3}$ are consistent with conventional working stress design methods using $FS = 2.0 - 3.0$ except in cases where there is very high coefficient of variation, $COV_{s_u} \geq 0.8$ and/or small correlation ratios, $\Theta_{\ln s_u} < 1$.

Acknowledgment

The Authors are grateful to the Japanese Ministry of Education (MEXT) for providing Post-Doctoral support to the first Author at MIT.

References

Baecher, G.B. & Christian, J.T. (2003) *Reliability and statistics in geotechnical engineering*, John Wiley & Sons, Ltd., NY, 605p.

DeGroot, D.J. & Baecher, G.B. (1983) "Estimating autocovariance of in situ soil properties," *ASCE J. Geotech. Eng.*, 129(1), 147-166.

Fenton, G. A., and Vanmarcke, E. H. (1990). ''Simulation of random fields via local average subdivision.'' *J. Eng. Mech.,* 116(8), 1733-1749.

Griffiths, D. V., and Fenton, G. A. (2001). "Bearing capacity of spatially random soil: The undrained clay Prandtl problem revisited." *Geotechnique*, 51(4), 351-359.

Griffiths, D. V., Fenton, G. A., and Manoharan, N. (2002). "Bearing capacity of rough rigid strip footing on cohesive soil: probabilistic study." *ASCE J. Geotech. Eng.*, 128(9), 743-755.

Lyamin, A.V. & Sloan, S.W. (2002a) "Lower bound limit analysis using non-linear programming," *Intl. Journal for Numerical Methods in Engineering*, 55(5), 573-611.

Lyamin, A.V. & Sloan, S.W. (2002a) "Upper bound limit analysis using finite elements and non-linear programming," *Intl. Journal for Numerical and Analytical Methods in Geomechanics*, 26(2), 181-216.

Phoon, K.K. & Kulhawy, F.H. (1999) "Characterization of geotechnical variability," *Canadian Geotechnical Journal*, 36, 612-624.

Phoon, K.K., Kulhawy, F.H. & Grigoriu, M.D. (2000) "Reliability-based design for transmission line structure foundations," *Computers & Geotechnics*, 26, 169-185.

Sloan, S. W. (1988a). "Lower bound limit analysis using finite elements and linear programming." *Int. J. Numer. Analyt. Meth. Geomech.*, 12(1), 61-77.

Sloan, S. W. (1988b). "A steepest edge active set algorithm for solving sparse linear

programming problems." *Int. J. Numer. Analyt. Meth. Geomech.*, 12(12), 2671-2685.

Sloan, S. W., and Kleeman, P. W. (1995). "Upper bound limit analysis using discontinuous velocity fields." *Comput. Methods Appl. Mech. Eng.*, 127, 293-314.

Ukritchon, B., Whittle, A. J., and Sloan, S. W. (1998). "Undrained limit analyses for combined loading of strip footing on clay." *J. Geotech. Eng.*, 124(3), 265-276.

Vanmarcke, E. H. (1984). *Random fields: Analysis and synthesis*. MIT press, Cambridge, Mass.

NOTATION

B = width of foundation;

COV_{c_u} = coefficient of variation of undrained shear strength;

s_u = undrained shear strength;

s_{u_i} = undrained shear strength of ith element;

FS = safety factor;

$G(x)$ = standard Gaussian field with zero mean unit variance;

$G(x_i)$ = local value of standard Gaussian field with zero mean unit variance for ith element;

N_c = bearing capacity factor;

N_{c_i} = bearing capacity factor for i^{th} realization;

$P[\ldots]$ = probability;

$\boldsymbol{x}_i$ = position vector at center of i^{th} element;

$\Theta_{\ln s_u} = \theta_{\ln s_u} / B$, dimensionless correlation length ratio,;

$\theta_{\ln s_u}$ = spatial correlation length;

μ_{s_u} = mean undrained shear strength;

$\mu_{\ln s_u}$ = mean of log undrained shear strength;

$\mu_{\ln N_c}$ = mean of log bearing capacity factor;

μ_{N_c} = mean bearing capacity factor;

ρ = correlation coefficient;

σ_{s_u} = standard deviation of undrained shear strength;

$\sigma_{\ln s_u}$ = standard deviation of log undrained shear strength;

$\sigma_{\ln N_c}$ = standard deviation of log bearing capacity factor;

σ_{N_c} = standard deviation of bearing capacity factor;

$\Phi(...)$ = cumulative normal function.

LIST OF FIGURES

LIST OF TABLES

Table 1. Bearing capacity factor statistics and goodness of fit results for normal and log-normal distributions

$\Theta_{\ln c_u}$	COV_{c_u}	LB						UB					
		μ_{N_c}	σ_{N_c}	χ^2	$\mu_{\ln N_c}$	$\sigma_{\ln N_c}$	χ^2	μ_{N_c}	σ_{N_c}	χ^2	$\mu_{\ln N_c}$	$\sigma_{\ln N_c}$	χ^2
0.1	0.2	4.330	0.082	22.2	1.465	0.019	24.3	4.815	0.099	27.1	1.572	0.021	22.3
	0.4	3.572	0.127	20.2	1.272	0.036	19.2	4.16	0.171	24.5	1.425	0.041	24.2
	0.6	2.858	0.154	24.0	1.049	0.054	27.2	3.472	0.217	22.8	1.243	0.062	27.3
	0.8	2.353	0.145	21.3	0.854	0.061	25.1	2.937	0.208	22.3	1.075	0.07	15.1
	1.0	1.921	0.157	14.2	0.649	0.084	10.4	2.467	0.238	22.3	0.898	0.099	24.1
	4.0	0.375	0.070	22.3	-0.998	0.192	22.8	0.555	0.119	17.8	-0.613	0.224	11.9
0.2	0.2	4.425	0.108	24.9	1.487	0.024	21.2	4.821	0.126	22.4	1.573	0.026	26.4
	0.4	3.737	0.178	27.4	1.317	0.047	16.6	4.215	0.225	14.4	1.437	0.053	24.5
	0.6	3.053	0.257	20.8	1.112	0.085	16.7	3.512	0.375	18.7	1.250	0.108	24.2
	0.8	2.545	0.247	21.2	0.929	0.098	26.1	2.986	0.345	21.2	1.087	0.117	23.7
	1.0	2.146	0.257	26.8	0.756	0.126	19.3	2.580	0.352	26.7	0.938	0.145	14.7
	4.0	0.449	0.112	26.7	-0.835	0.268	22.8	0.591	0.168	13.7	-0.570	0.308	15.8
1	0.2	4.617	0.238	14.4	1.528	0.052	15.1	4.788	0.301	25.3	1.564	0.063	25.2
	0.4	4.033	0.512	21.5	1.386	0.132	20.3	4.187	0.584	26.5	1.422	0.144	27.2
	0.6	3.541	0.568	15.1	1.250	0.173	24.8	3.701	0.645	22.7	1.292	0.191	20.7
	0.8	3.155	0.589	14.5	1.127	0.229	26.2	3.241	0.682	12.9	1.148	0.253	21.0
	1.0	2.721	0.722	21.1	0.958	0.312	17.9	2.807	0.833	15.0	0.979	0.349	17.7
	4.0	0.877	0.589	27.6	-0.405	0.730	21.0	0.899	0.663	25.1	-0.346	0.809	19.0
2	0.2	4.731	0.260	22.7	1.553	0.056	15.0	4.860	0.307	16.2	1.579	0.064	20.4
	0.4	4.278	0.476	15.7	1.447	0.120	26.8	4.342	0.539	25.1	1.460	0.132	15.2
	0.6	3.785	0.609	24.1	1.317	0.175	24.4	3.823	0.722	21.3	1.321	0.205	20.4
	0.8	3.418	0.758	18.4	1.202	0.244	26.4	3.457	0.860	17.9	1.206	0.275	26.2
	1.0	3.102	0.849	12.2	1.084	0.289	22.5	3.137	0.935	11.2	1.104	0.318	18.7
	4.0	1.417	0.805	27.1	0.126	0.644	21.9	1.503	0.899	26.7	0.230	0.710	16.7
4	0.2	4.825	0.185	25.0	1.573	0.038	25.0	4.940	0.225	9.7	1.596	0.046	10.6
	0.4	4.522	0.369	21.1	1.506	0.083	22.7	4.605	0.461	21.4	1.522	0.103	14.3
	0.6	4.235	0.512	18.6	1.436	0.125	21.5	4.318	0.606	20.4	1.452	0.146	23.3
	0.8	3.698	0.726	23.5	1.280	0.216	24.5	3.703	0.822	20.2	1.288	0.245	24.4
	1.0	3.478	0.801	20.6	1.206	0.262	21.2	3.496	0.904	25.3	1.221	0.299	25.8
	4.0	1.958	0.938	22.1	0.512	0.576	21.6	1.976	0.973	22.3	0.541	0.627	22.9
8	0.2	4.894	0.170	20.6	1.587	0.035	15.0	5.022	0.189	18.9	1.613	0.038	21.1
	0.4	4.676	0.317	25.6	1.540	0.069	18.6	4.739	0.399	19.2	1.552	0.087	21.9
	0.6	4.432	0.431	24.8	1.484	0.099	18.7	4.485	0.534	21.5	1.494	0.121	12.1
	0.8	4.140	0.652	17.4	1.407	0.166	24.8	4.200	0.77	15.2	1.417	0.195	16.2
	1.0	3.882	0.610	21.9	1.341	0.166	14.1	3.894	0.721	14.7	1.343	0.193	18.7
	4.0	2.773	0.925	16.4	0.936	0.388	19.6	2.817	1.034	19.2	0.970	0.441	14.8
20	0.2	4.938	0.113	8.2	1.597	0.023	9.9	5.085	0.137	25.0	1.626	0.027	26.5
	0.4	4.845	0.226	20.6	1.577	0.047	24.8	4.945	0.278	27.5	1.597	0.056	25.2
	0.6	4.688	0.312	26.0	1.543	0.068	21.7	4.762	0.392	23.3	1.557	0.082	14.0
	0.8	4.530	0.381	7.9	1.507	0.085	16.5	4.584	0.470	25.1	1.517	0.102	24.0
	1.0	4.454	0.431	13.2	1.489	0.101	15.9	4.506	0.511	10.8	1.499	0.113	15.5
	4.0	3.468	0.783	16.7	1.209	0.235	26.9	3.503	0.880	18.7	1.227	0.250	17.8

Note: Acceptance criterion $\chi^2_{20\text{-}1\text{-}2}[0.05] \leq 27.6$

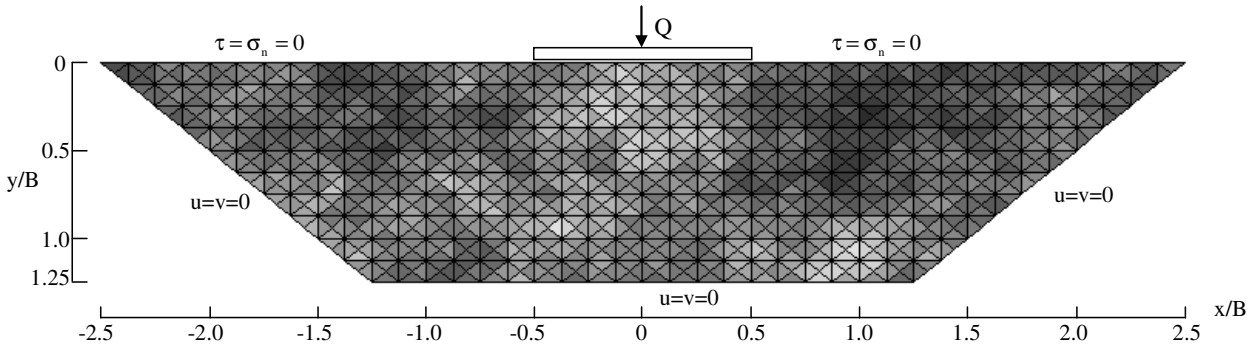

Fig. 1. Typical finite element meshes used in numerical limit analyses for rough strip footing (COV_{s_u}=0.2, $\Theta_{\ln s_u}$=1)

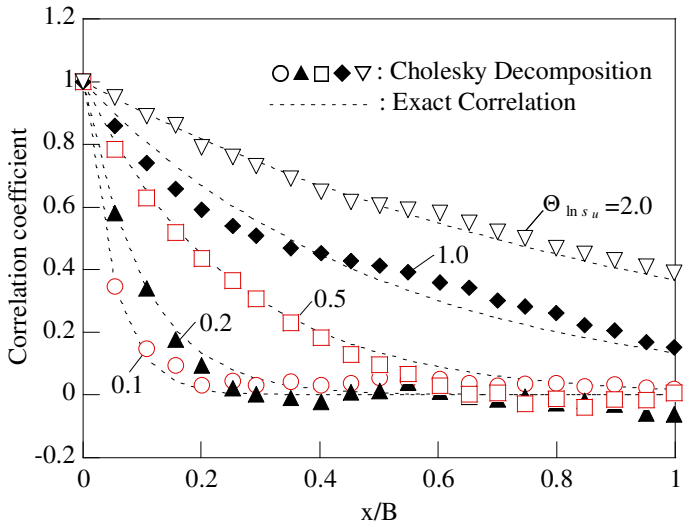

Fig. 2. Comparison of exact correlation relation and realized correlation obtained by Cholesky Decomposition technique

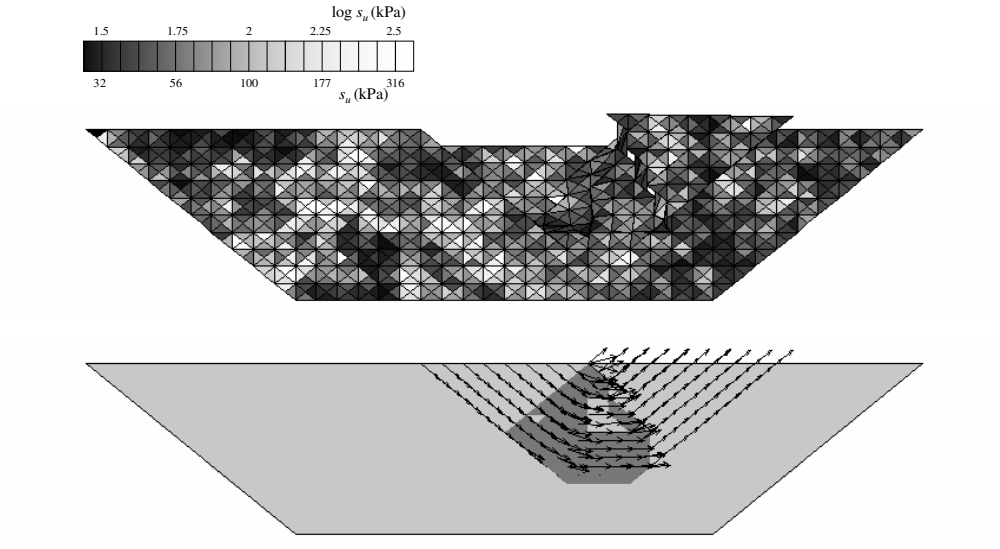

a) COV_{s_u} =0.4, $\Theta_{\ln s_u}$ =0.2

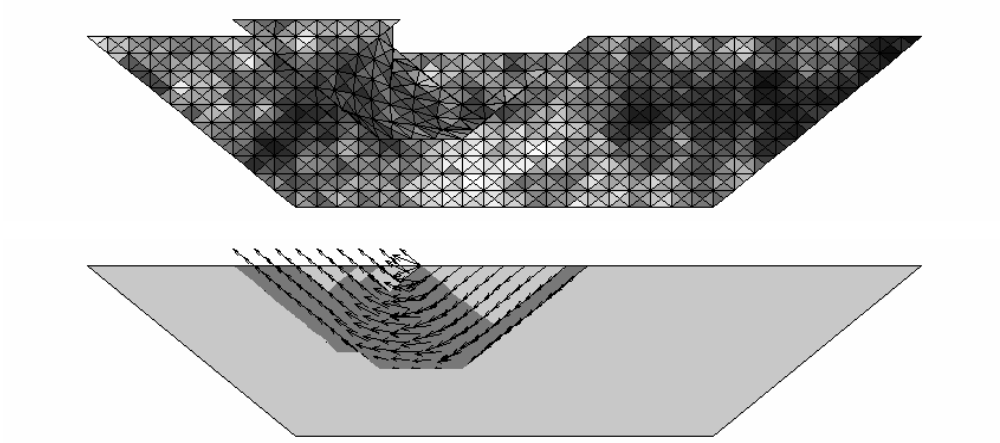

b) COV_{s_u} =0.4, $\Theta_{\ln s_u}$ =1

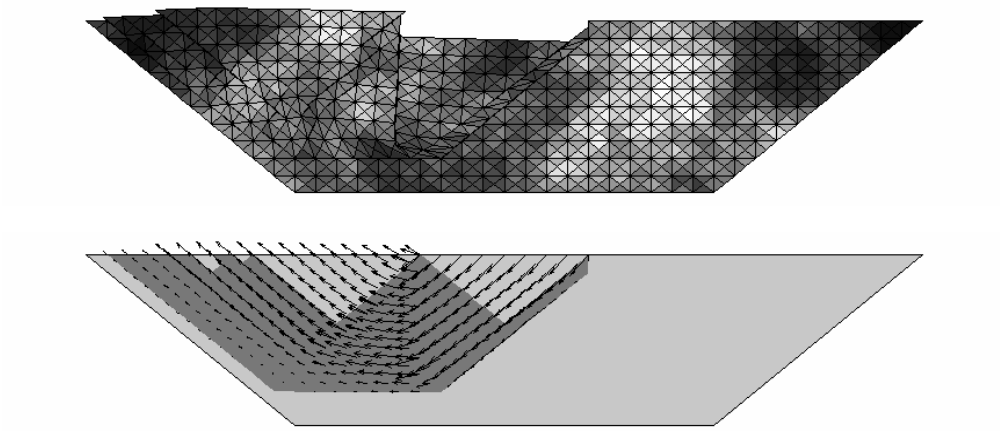

c) COV_{s_u} =0.4, $\Theta_{\ln s_u}$ =2

Fig. 3. Typical results of Upper Bound Analyses

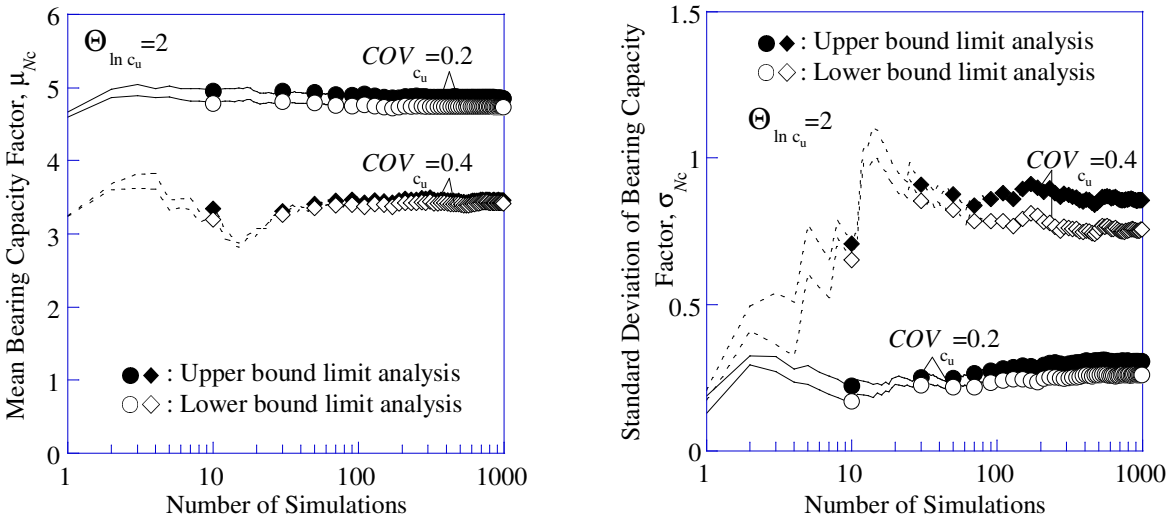

a) Mean bearing capacity factor b) Standard deviation of bearing capacity factor

Fig. 4. Bearing capacity factor against number of simulations

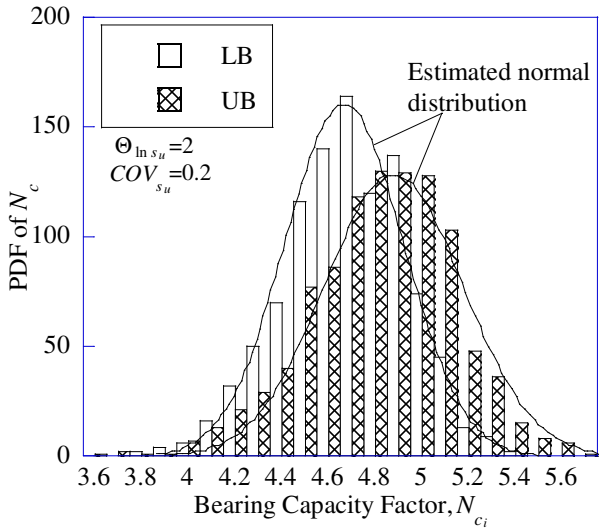

Fig. 5. Histogram and estimated normal distribution of bearing capacity factor

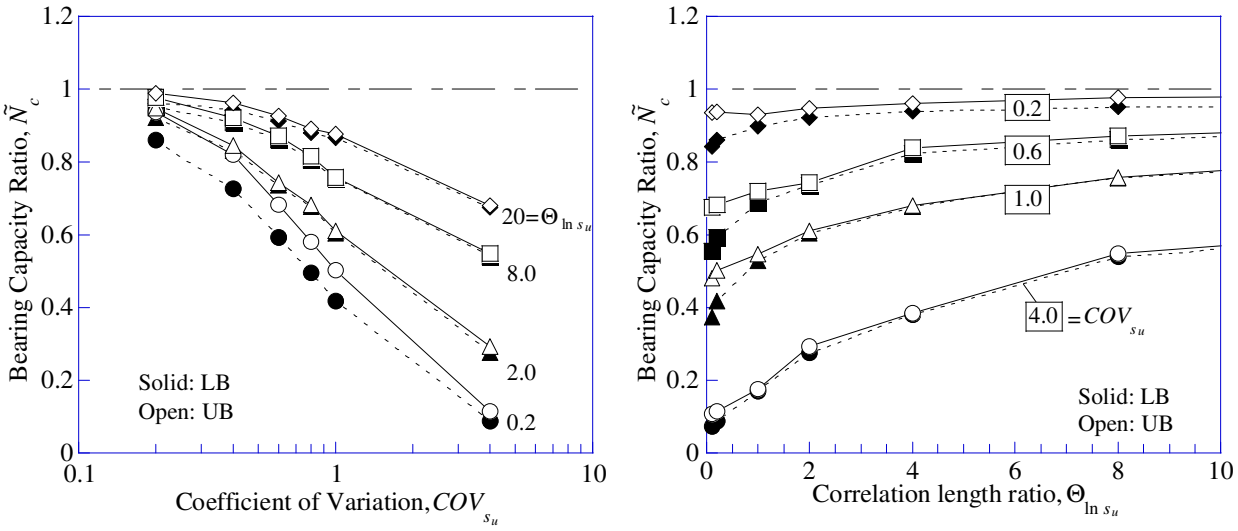

a) factor of COV_{s_u}

b) factor of $\Theta_{\ln s_u}$

Fig. 6. Summary of mean bearing capacity ratio $\tilde{N}_c$

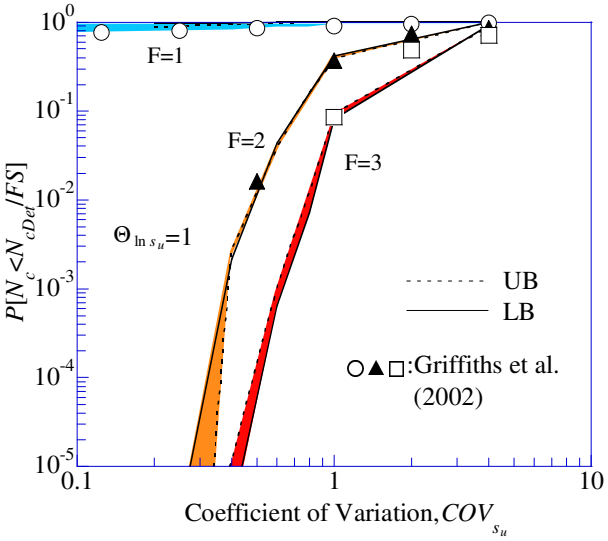

a) $\Theta_{\ln s_u}$=1

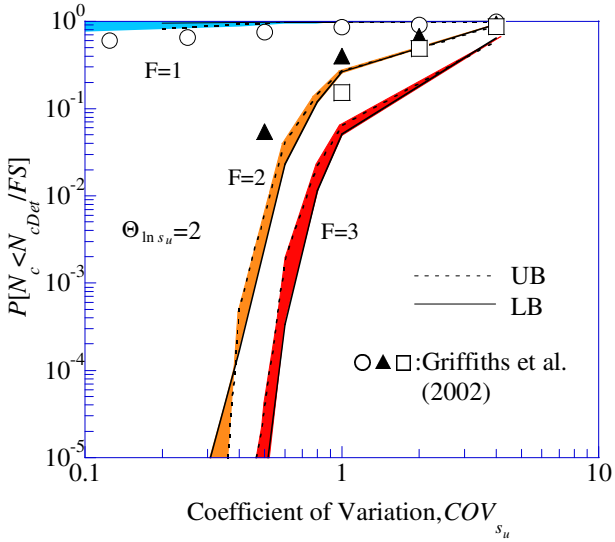

b) $\Theta_{\ln s_u}$=2

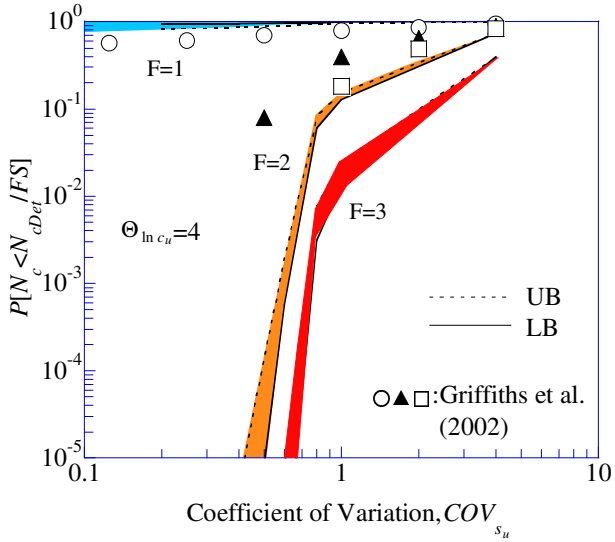

c) $\Theta_{\ln s_u}$=4

Fig. 7. Probability that the bearing capacity factor is less than the nominal design load

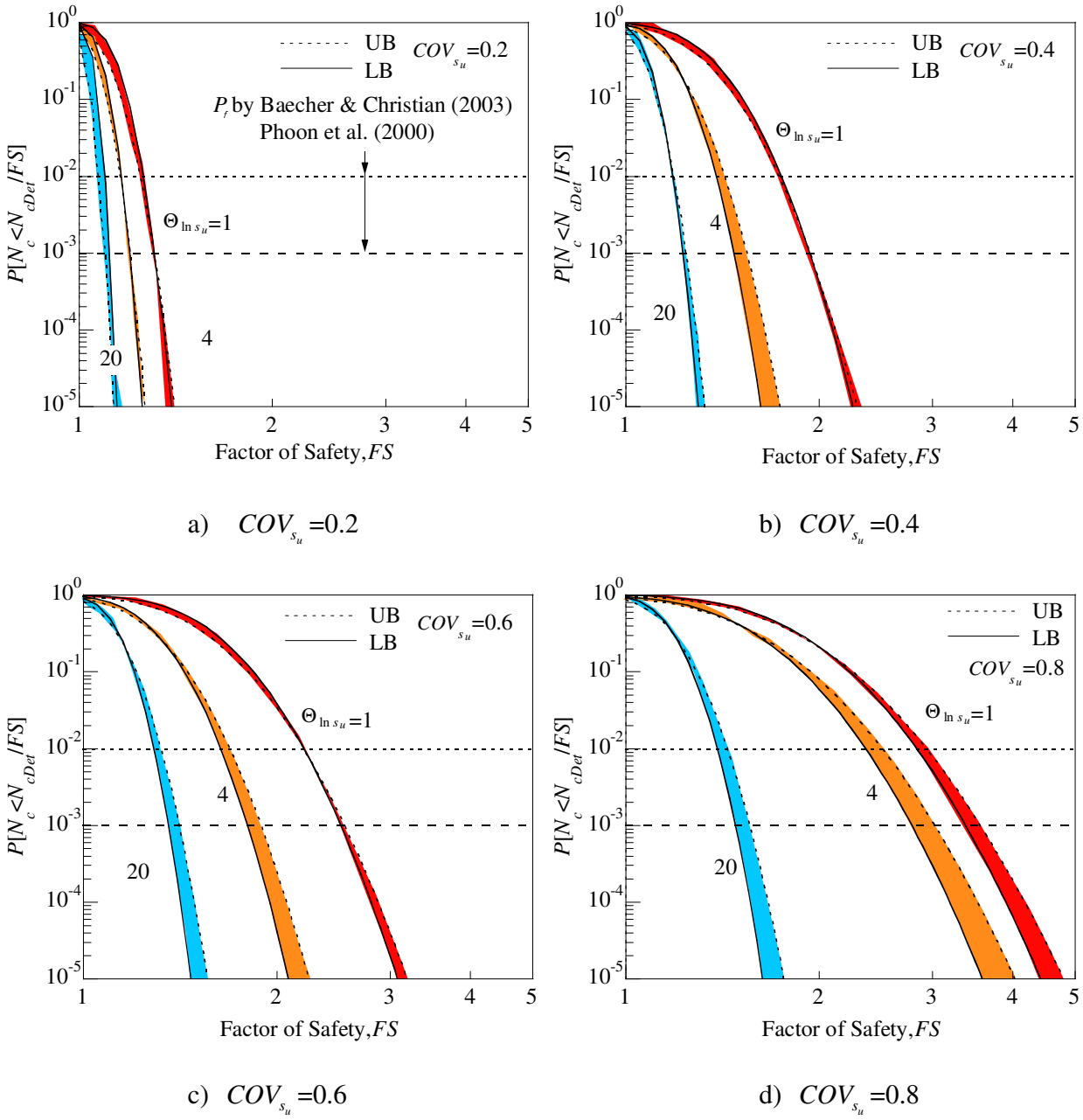

Fig. 8. Comparison of failure probability and conventional safety factor